Functional Materials 12, No.1 (2005)

Influence of oxide layers on optical properties of copper in a wide spectral range

Y.V.Filipov, V.S.Staschuk, L.V.Poperenko

Department of Physics, T.Shevchenko National Kyiv University,
6 Acad. Glushkov Ave., 03127 Kyiv, Ukraine

Optical properties of flawless bulk copper sample has been studied based on spectroellipsometry measurements in a wide spectral interval ($h\nu$ = 0.18 to 4.87 eV) at various angles of light incidence. The main characteristics of electronic subsystem of this metal and values of main energy intervals in a band structure have been calculated. Taking into consideration influence of the surface oxide layer.

Исследованы оптические свойства массивных образцов меди с идеальной структурой на основе спектроэллипсометрических измерений в широкой области спектра ($h\nu$ = 0.18–4.87 эВ) при различных углах падения света. Рассчитаны характеристики электронной подсистемы металла и основные энергетические интервалы зонной структуры медных образцов с учетом влияния поверхностного слоя окиси.

Light wave reflected from a metal is formed due to interaction of the incident wave with the electronic subsystem of the material surface layer. For example, for copper in the visible range, that layer is about 3.0–4.5 nm thick [1]. Since a metal sample in normal conditions is coated with an oxide layer [2], it is necessary to take into consideration the influence of such surface oxide layer on the reflectivity determined for pure metal.

Optical properties of copper were studied most comprehensively as compared to other metals. This interest is defined by several factors. First, it is possible to obtain a copper sample of high purity up to 99.9995 %. Second, the objects made of this metal are easy to process and, therefore, to obtain samples with very high surface quality. Third, the electronic structure of copper is studied, rather well its *d* bands are completely occupied and placed approximately 2.1–2.2 eV below the Fermi level [3]. Fourth, copper is widely used in practice. Though many works are dedicated to the research of optical properties of copper [4], those properties have not been studied completely. The majority of researches was made in narrow spectral ranges [5] and their results do not coincide with each other, therefore, do not give complete information on the nature of interband transitions. Our purpose was to study the electronic structure of flawless unoxidized bulk copper basing on measurements of optical constants n and κ within a wide spectral range of intraband and interband absorption.

To that end, the phase shift Δ and azimuth ψ of the restored linear polarization in a wide spectral range of light wavelengths λ = 0.25 to 7 μm ($h\nu$ = 0.18 to 4.87 eV) were measured at room temperature. The reflective surfaces of copper samples were made by mechanical grinding and polishing of bulk copper of 99.999 % purity using recrystallization annealing and electrolytic polishing. By measuring Δ and ψ at multiple angles φ of light incidence and solving the inverse problem of ellipsometry [6], it is established for single-layer model that an oxide layer of 4.2 nm thickness is present at the copper sample surface. This value was used to calculate the optical constants of unoxidized metal. The results of the measurements and calculations of refractive indices n and absorption æ are presented in Fig. 1. In the ultra-

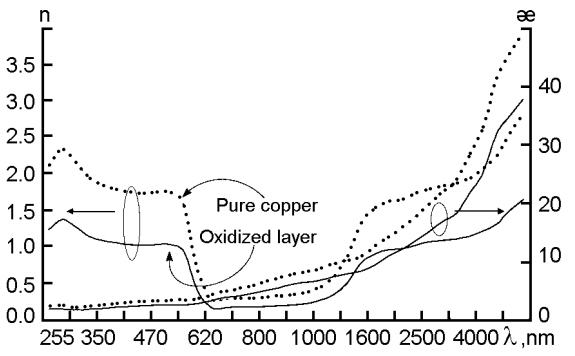

Fig. 1. Indices of refraction n and absorption æ for a copper sample.

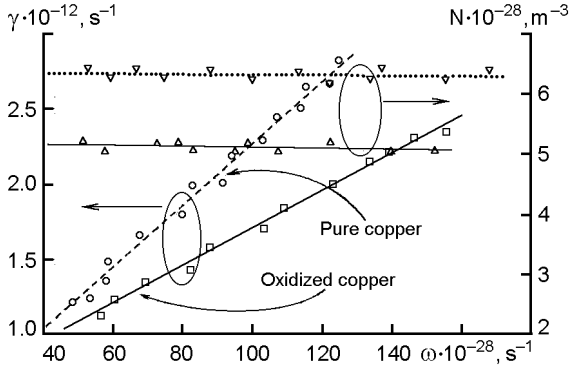

Fig. 2. Electron density N and electron collision frequency γ for a copper sample.

violet, the absorption values for metal and copper monoxide are comparable, therefore, the oxide layer influence can be neglected. From Fig. 1, it is seen that the reduction of the mentioned indices for an oxidized layer is rather essential in the whole measured range and within some spectral intervals it makes more than 30 % (κ) and 70 % (n) decrease. The analysis of the dispersion relations demonstrates that in the infrared at $h\nu < 1.5$ eV, the intraband transitions dominate, while within photon energy range $h\nu > 1.9$ eV, the interband electron transitions are observed.

The detailed analysis of the obtained data and their correlation with theoretical background results in a conclusion that light absorption by the conduction electrons at photon energies $h\nu < 1.2$ eV may be due to a weak anomalous skin effect. Applying the iterative method to the scheme designed in [7], the free electron collision frequency γ and free electron density N were determined. It was found that the density N is frequency-independent as it has to be expected, while the electron collision frequency γ depends strongly on frequency. The calculated values N and γ are shown in Fig. 2. In the $h\nu$ range of 0.3 to 0.83 eV, the relationship of electron collision frequency γ is described by linear dependence on the square of frequency ω for both oxidized and unoxidized copper. This testifies a strong influence of electron interconnection on the electron collision frequency [8]. Nevertheless, it is necessary to take into account that even at room temperature, in flawless copper samples with perfect structure electron-photon collisions take place. The correct separation among the contributions of electron-electron and electron-photon collisions in copper is possible only after measurements of optical parameters within a wide temperature interval. In the λ range of 1.5 to 6 μm, the free electron density N is essentially independent of the light wavelength, thus evidencing the adequacy of the selected surface model for calculation of electronic characteristics. The values $N = 4.25 \cdot 10^{28}$ and $6.37 \cdot 10^{28}$ m^{-3} for oxidized and unoxidized copper sample, respectively, differ by a factor more than 1.5.

The most informative analysis of the copper electronic characteristics is provided by consideration of the separated spectra of interband optical conductivity obtained from experimental optical conductivity spectra computed basing on spectroellipsometrical measurements data in the relaxation range of conduction electrons. The relevant characteristic among appropriate optical parameters is optical conductivity $\sigma = n\kappa\nu$ since this value is proportional to the combined interband density of electron states [9]. The dependence of optical conductivity σ on photon energy $h\nu$ for oxidized and unoxidized copper sample is shown in Fig. 3. It is seen that within the range 1 to 4 eV, the of absorption band edge for unoxidized and oxidized copper sample lies at $h\nu = 2.6$ and 2.45 eV, respectively. At the same time, the intensity of appropriate maximum in the $\sigma(h\nu)$ spectrum is almost twice higher than that for oxidized copper sample.

Using results of data interpretation in the IR which allow to determine the electron characteristics, it is possible to dedicate the contribution $\tilde{\sigma}$ of the interband transitions to optical conductivity σ [10]

$$\tilde{\sigma}(\omega) = \sigma(\omega) - \frac{1}{4\pi} \frac{\Omega^2 \gamma}{\omega^2 + \gamma^2},$$

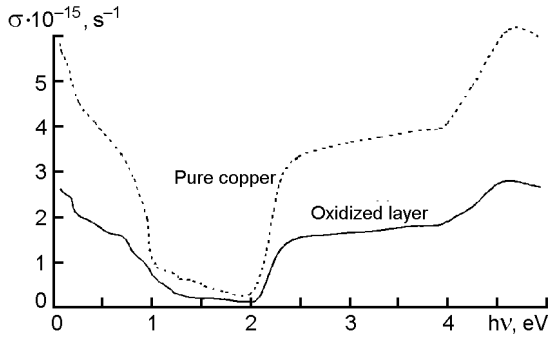

Fig. 3. Dependence of optical conductivity σ on photon energy $h\nu$ for oxidized and unoxidized copper sample.

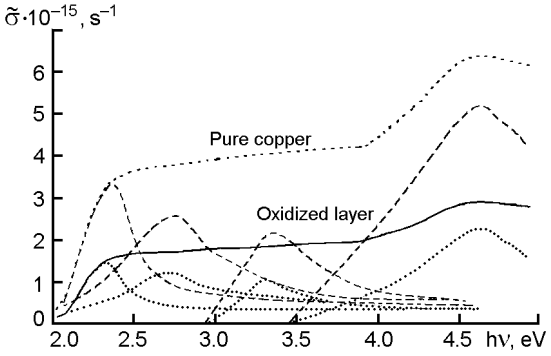

Fig. 4. Interband optical conductivity for oxidized and unoxidized copper sample.

where Ω is the plasma frequency and γ is free electron collision frequency.

The dispersion curves $\tilde{\sigma}(h\nu)$ of interband optical conductivity for oxidized and unoxidized copper sample are shown in Fig. 4. It is seen that the copper monoxide layer distorts the the absorption curve shape and results in a shift of its maximum by 0.2 eV towards longer wavelengths. The detailed analysis of the obtained results and their comparison with theoretical data has shown that the main absorption band has complex structure and consists of several components. It is necessary to note that the structure of the absorption bands is more pronounced in curve $\tilde{\sigma}$ ($h\nu$) for unoxidized copper sample. The results obtained for the interband absorption are described using the electron band structure approach [11]. In Fig. 5, the band structure of copper are shown and possible interband transitions forming the absorption spectrum are indicated by arrows. The absorption edge at $h\nu$ = 2.25 eV is formed with respect to direct transitions near L and X points of the Brillouin zone. This absorption in copper is boosted while photon energy increases and characteristic "plateau" is formed in appropriate spectrum. A lower absorption is connected with interband transitions from top of d-like bands to p-like band in L-Q-W direction of the Brillouin zone. The interband transitions from d-like states to p-like one are realized in X point of the Brillouin zone at photon energy of approximately 3.5 eV. The broad maximum at $h\nu$ = 4.6 eV is due to interband transitions at W point of the Brillouin zone. These results specify existing data on electronic spectrum of copper [12].

A detailed consideration of the obtained results in the intraband absorption range has given other parameters which characterize the electronic system of copper. To that end, the relationships can be used associating the optical characteristics of copper with main parameters of its conduction electron system. In particular, we have calculated the valence electron density N_{val} and velocity V_F^0 of free electrons at the Fermi surface. These values can be calculated using well-known equations of classic electronic theory [13]

$$N_{val} = \frac{N_A d}{\mu}, \quad V_F^0 = \frac{\hbar}{m}(3\pi^2 N_{val})^{1/3},$$

where N_A is the Avogadro constant; μ –atomic mass of copper; d–density of copper; and m–the mass of free electron.

These data together with ones obtained before allow us to calculate the average value $\overline{V}_F$ of electron velocity at the Fermi surface. For this purpose, the following relation can be used [14]:

$$\frac{\overline{V}_F}{V_F^0} \approx \sqrt{\frac{N}{N_{val}}} \approx \frac{S_F}{S_F^0},$$

where S_F and S_F^0 are the squares of real Fermi surface of copper and spherical Fermi surface for valence electrons in free electron approximation, respectively.

The main parameter of the electronic subsystem is the electron effective mass m^* which can be estimated in pseudopotential approximation. It is possible to use the relation which is similar to the above-mentioned ones, defining the value $N^* = Nm^*/m_e$. Then the values S_F and V_F may be connected with free electron density N^* by the following relation:

$$S_F = S_F^0\sqrt{\frac{N_{val}}{N^*}}, \quad V_F = V_F^0\sqrt{\frac{N_{val}}{N^*}}.$$

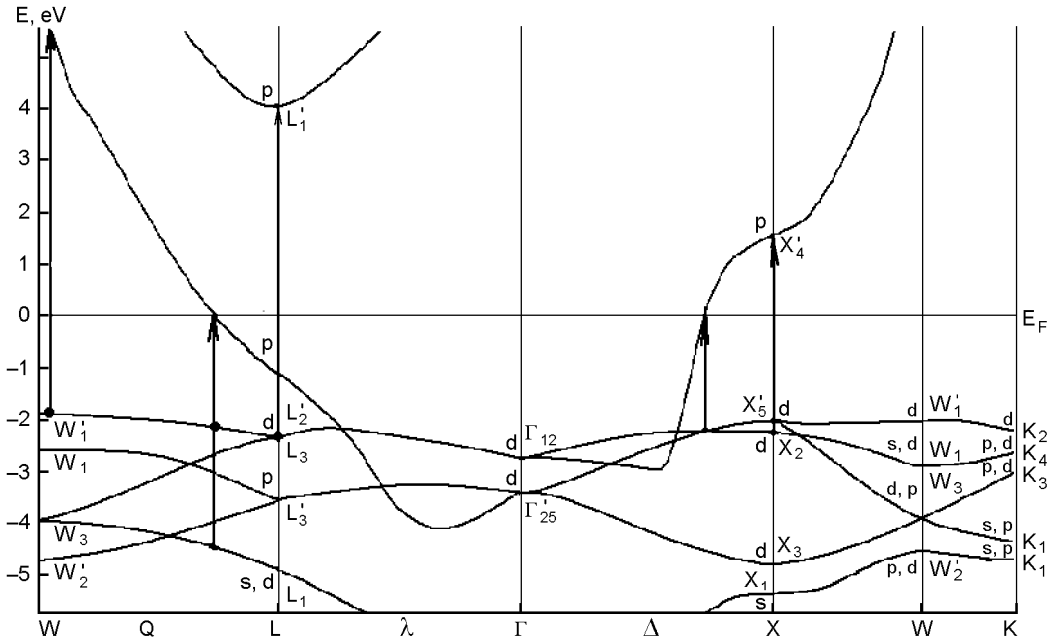

Fig. 5. The band structure of copper.

From these relations, it is possible to get the expression for effective mass of conduction electron

$$m^* = m_e\sqrt{\frac{N_{val}}{N}}.$$

Basing on experimental N values for oxidized and unoxidized copper sample and the obtained valence electron density $N_{val} = 8.57{\cdot}10^{28}$ m^{-3}, it is found that $m^* = 1.42\ m_e$ and $1.1\ m_e$ for oxidized and unoxidized copper, respectively. That is why the effective electronic mass for copper does not strongly differ from the free electron one and this fact is characteristic for other noble metals [15].

Then the values of the electron free path l and depth δ of skin layer were obtained from the following relationships [16]:

$$l = \frac{\overline{V}_F}{\gamma}, \quad \delta = \frac{\lambda}{2\pi\kappa}.$$

In the range of $\lambda > 6$ μm, the electron free path l and skin-layer depth δ become values of the same order. In this case, the skin-effect becomes anomalous, and to process the numerical values of the mentioned quantities, it is necessary to use only the results of the theory of anomalous skin effect.

The obtained characteristics are tabulated in the Table below.

It is seen that some results for unoxidized copper differ more than by 1.5 times as compared to those for oxide layer while other results are almost the same.

Basing on the data obtained, it is possible to calculate the value of plasma oscillations frequency $\Omega = e\sqrt{4\pi N/m} = e\sqrt{4\pi N^*/m^*} = 1.16{\cdot}10^{16}$ s^{-1} and $\Omega = 1.51{\cdot}10^{16}$ s^{-1} for oxidized and unoxidized copper, respectively.

As a conclusion, the results obtained for unoxidized copper sample are agree better with the theoretical calculations. The oxide layer on a copper mirror surface influences essentially on its optical reflectivity that results in distorted data on electronic structure of this metal. Thus, the measurement of optical constants for copper in wide spectral range at various angles of light incidence on metal made it possible to deter-

Table

Oxide layer, nm	N^*, 10^{28} m^{-3}	N^*/N_{val}	V_F^*, 10^6 m/s	S_F^*, 10^{-47} kg^{2}m^2/s^2	m^*/m_e	l, 10^{-8}m (λ = 3 μm)	δ, 10^{-8}m (λ = 3 μm)	Ω, 10^{16} s^{-1}
4.2	6.02	0.707	1.32	2.17	1.42	2.32	2.60	1.16
0	7.76	0.911	1.42	2.33	1.10	2.21	2.03	1.51

mine some characteristics of electronic subsystem of this metal such as mass, density and velocity of electrons at the Fermi surface. The values of main energy intervals in the metal band structure responsible for characteristic spectrum structure of the interband absorption for both oxidized and unoxidized copper sample are also reliably determined.

References

1. Y.V.Filipov, V.S.Staschuk, L.V.Poperenko, *Semiconductor Physics, Quantum Electronics & Optoelectronics*, **7**, 287 (2004).
2. H.Arwin, D.E.Aspnes, *Thin Solid Films*, **138**, 195 (1986).
3. A.K.Ahnja, S.Auluck, S.K.Joshi, *Phys. Stat. Sol.*, **118**, 575 (1983).
4. H.Erenreich, H.R.Phillipp, *Phys. Rev.*, **128**, 1622 (1962).
5. T.P.Blaulac, P.B.Alen, *Phys. Rev.*, **26**, 1549 (1982).
6. H.G.Tompkins, W.A.McGahan, Spectroscopic Ellipsometry and Reflectometry, J.Wiley, New York (1999).
7. A.Mookerjee, R.Prasad, *Phys. Rev.*, **48**, 725 (1993).
8. U.Geiersbach, A.Bergmann, K.Westerholt, *J. Magn. and Magn. Mater.*, **240**, 546 (2002).
9. Handbook of Optical Constants of Solids, ed. by D.E.Palik, Academic Press, New York (1997).
10. M.M.Noskov, Optical and Magnetooptical Properties of Metals, Sverdlovsk (1983) [in Russian].
11. T.Saha, I.Dasgupta, A.Mookerjee, *Phys. Rev.*, **50**, 267 (1994).
12. M.Lindroos, H.Asonen, M.Pessa, *Sol. State Comm.*, **39**, 285 (1981).
13. W.A. Harrison, Solid State Theory, McGraw, New York (1970).
14. C. Kittel, Introduction to Solid State Physics, New York (1967).
15. Handbook of the Elements, ed. by B.V. Crist, XPS International, New York (1999).
16. G.P.Motulevich, *Trudy FIAN*, **55**, 3 (1971).

Вплив оксидного шару на оптичні властивості міді у широкій області спектру

Я.В.Філіпов, В.С.Стащук, Л.В.Поперенко

Досліджено оптичні властивості масивних мідних зразків з ідеальною структурою на основі спектроеліпсометричних досліджень у широкій області спектру ($h\nu$ = 0.18–4.87 еВ) при варіюванні кута падіння світла. Розраховано характеристики електронної підсистеми металу та основні енергетичні інтервали зонної структури мідних зразків з урахуванням впливу приповерхневого шару оксиду.